^{1}H NMR Study of the Solution Molecular and Electronic Structure of *Escherichia coli* Ferricytochrome b_{562}: Evidence for $S = {}^1/_2 \rightleftharpoons S = {}^5/_2$ Spin Equilibrium for Intact His/Met Ligation†

Jia-zhen Wu, Gerd N. La Mar,* Liping P. Yu, and Kang-Bong Lee
Department of Chemistry, University of California, Davis, California 95616
F. Ann Walker‡
Department of Chemistry, San Francisco State University, San Francisco, California 94132
Mark L. Chiu and Stephen G. Sligar
Department of Biochemistry, University of Illinois, Urbana, Illinois 61801
Received August 13, 1990; Revised Manuscript Received November 6, 1990

ABSTRACT: The solution 500-MHz ^{1}H NMR spectral parameters for ferricytochrome b_{562}, a soluble 12-kDa electron carrier from *Escherichia coli* with axial His/Met coordination, are shown to be strongly influenced by protein concentration and ionic strength at low pH and 25 °C in a manner consistent with significant aggregation at low ionic strength. At high ionic strength a well-resolved ^{1}H NMR spectrum reveals over 40 hyperfine-shifted resonances which arise from two isomeric species in the ratio 2:1. 2D COSY and NOESY maps at 25 °C for the hyperfine-shifted resonances allow the assignment of a number of axial His resonances and all heme peripheral substituent peaks. The resulting asymmetric heme contact shift patterns, together with the halving of the number of lines when reconstituting with 2-fold symmetric hemin, demonstrate the molecular basis of the solution heterogeneity to be heme orientational disorder. The strongly upfield-shifted axial Met-7 resonances, characteristic of low-spin ferricytochromes *c* with His/Met ligation, appear upfield only at very low temperatures. At elevated temperatures, all resonances, in particular those of the axial Met, move strongly downfield. Detailed analysis of the deviation from Curie behavior for different functional groups demonstrates the presence of a low spin $\rightleftarrows$ high spin equilibrium with an intact His–Fe–Met coordination. The weaker axial field in ferricytochrome b_{562}, relative to the purely low-spin ferricytochromes *c*, is attributed to a perturbed iron–Met bond. The contact shifts for a coordinated Met in the high-spin state are estimated. A link between equatorial hemin and axial ligand interactions is indicated by a differential population of the high-spin form for the two hemin orientations.

Cytochrome b_{562} is a small (12-kDa) soluble electron carrier isolated from cell extracts from *Escherichia coli* (Hager & Itagaki, 1967). Although it is a likely functional analogue to cytochrome *c* (Dickerson & Timkovitch, 1975), it exhibits little sequence homology to the more common classes of cytochromes *c* and possesses a labile protohemin prosthetic group (Itagaki & Hager, 1966). The oxidized form of the protein has been proposed to be low spin (Bullock & Myer, 1978). An X-ray crystal structure of ferricytochrome b_{562} revealed an unusual folding pattern of a twisted barrel of four nearly parallel helices with the partially exposed hemin inserted into the bundle near the carboxy terminus and coordinated by His-102 and Met-7 (Figure 1A) (Mathews et al., 1979; Lederer et al., 1981). Thus cytochrome b_{562} has both sequence (Meyer & Kamen, 1982) and structural (Weber et al., 1981) homology with the five-coordinate high-spin cytochrome *c'*. The remarkably simple four-helical folding pattern for both cytochrome b_{562} and cytochrome *c'*, together with their ability to completely reversibly thermally denature (Myer & Bullock, 1978; M. T. Fisher, H. Nikkila, R. Gennis, and S. G. Sligar, submitted for publication; L. B. Dugad, G. N. La Mar, and R. G. Bartsch, unpublished results), makes these proteins ideal candidates for detailed studies of protein folding (Ghelis & Yon, 1982).

The solution structure of cytochrome b_{562}, however, has been found to exhibit pronounced sensitivity to ionic strength and to undergo multiple pH-modulated transitions, one of which was initially proposed to involve a redox-linked ligation change (Myer & Bullock, 1978). The solution properties of cytochrome b_{562} have been probed by ^{1}H NMR[1] both for the reduced form, for which an axial Met was identified (Xavier et al., 1978), as well as for the oxidized form, which led to the proposal that the major acid → alkaline transition involved deprotonation of the His for an intact His–Fe–Met coordination geometry (Moore et al., 1985). More extensive structural analysis by ^{1}H NMR has not been practical because of the strong tendency for autoxidation of the reduced protein, the relatively poor spectral resolution provided by the oxidized protein relative to that typical of ferricytochromes *c* and *b*, and the general scarcity of the protein. This latter obstacle has really been overcome recently with the successful overexpression of the protein in *Escherichia coli* based on a cloned gene (Sligar et al., 1990), which affords not only sufficient material for detailed studies, but also the opportunity for

† This research was supported by grants from the National Science Foundation, DMB-88-03611, and the National Institutes of Health, GM-33775.
‡ Present address: Department of Chemistry, University of Arizona, Tucson, AZ 85721.

[1] Abbreviations: NMR, nuclear magnetic resonance; DSS, 2,2-dimethyl-2-silapentane-5-sulfonate; NOE, nuclear Overhauser effect; NOESY, nuclear Overhauser effect spectroscopy; COSY, correlated spectroscopy; M-COSY, magnitude COSY; CD, circular dichroism.

0006-2960/91/0430-2156$02.50/0

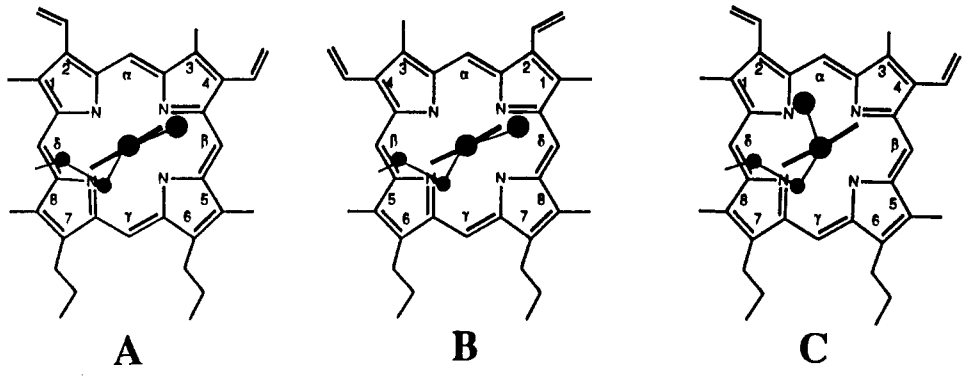

FIGURE 1: Schematic representation of the coordination geometry of protohemin with axial His-102 and Met-7 (imidazole projection indicated by a thick solid line) (large solid circles are bound sulfur and $C_\epsilon H_3$): (A) as found in the X-ray crystal structure of ferricytochrome b_{562} for which the axial Met has *R* chirality; (B) with the same Met-7 chirality as in the crystal structure, but with the hemin rotated 180° about the α,γ-meso axis; and (C) the X-ray orientation of the hemin, but with the *S* chirality of the axial Met-7.

manipulation of the structural and/or functional determinants of this interesting protein.

High-resolution ^{1}H NMR can be expected to provide a wealth of data on both solution structure and dynamic properties of the holoprotein (Wüthrich, 1986), as well as details of the pattern of unfolding of the native structure at elevated temperatures (Ghelis & Yon, 1982). Moreover, the exquisite sensitivity of the hyperfine interactions to even minor perturbations of the heme cavity molecular and/or electronic structure should provide information on temperature-dependent changes or structural constraints not readily detected in an analogous diamagnetic derivative (La Mar, 1979; Senn & Wüthrich, 1985; Satterlee, 1986). As a starting point for characterizing the reversible thermal unfolding of cytochrome b_{562}, we present herein a ^{1}H NMR study of the influences of solution conditions upon the electronic and molecular structure of the stable oxidized protein in the acidic or low-pH form, with emphasis on the resonances arising from the active site. We demonstrate that the previously reported ionic strength dependence of the CD spectral parameters (Myer & Bullock, 1978), as well as the inferior resolution of the previously reported ^{1}H NMR spectra (Moore et al., 1985), arises in large part form extensive solution dimerization of the protein. At high ionic strength, the ^{1}H NMR spectrum is extremely well resolved. As shown previously for the low-spin ferric hemoproteins cytochrome b_5 (McLachlan et al., 1988) and cyanometmyoglobin (Emerson & La Mar, 1990a), conventional 2D bond correlation spectroscopy or COSY (Bax et al., 1981) and nuclear Overhauser effect or NOESY (States et al., 1982) ^{1}H NMR methodology are directly applicable toward detailed assignment of the hyperfine-shifted resonances (Yu et al., 1990). The assignment of the heme resonances reveals extensive (2:1) heme orientational disorder and a thermal low-spin $\rightleftarrows$ high-spin spin equilibrium for intact His–Fe–Met bonding.

Experimental Procedures

Sample Preparation. Cytochrome b_{562} was prepared by using the cloned gene in an overproducing strain of *E. coli* (TB-1) carried in a pUC19 plasmic (Nikkila, 1987). Initial samples of the protein were harvested, isolated, and purified according to published procedures (Hager & Itagaki, 1967) to a ratio $A_{418}/A_{280} \sim 5.6$. Later samples of the protein (for the 2D NMR studies) were harvested, treated with chloroform to release periplasmic proteins (Ames et al., 1984), and then purified as follows: to 100 g of packed cells were added 100 mL of 0.1 M Tris buffer (pH 8.0) and 250 mL of $CHCl_3$. The resulting slurry was stirred 15 min and then centrifuged at 6000 rpm for 20 min. The chloroform layer and cell paste were extracted again as above with 100 mL of 0.1 M Tris buffer at pH 8.0. The orange supernatants from the two extractions were combined, and the pH was lowered to 5.0 with 0.5 M NaH_2PO_4. Unwanted denatured proteins were removed by centrifugation at 11000 rpm for 25 min. The orange supernatant was concentrated 3 times to ca. 50 mL with 50 mM phosphate at pH 4.55. Then a 15-mL portion was loaded onto a 2 × 25 cm CM52 ion-exchange column which had been equilibrated with 50 mM phosphate at pH 4.55. It was washed with 150 mL of 50 mM phosphate, by 100 mL of 50 mM NaCl/50 mM phosphate, and by 300 mL of a 50→150 mM NaCl/50 mM phosphate gradient solution, all at pH 4.55. Additional portions were run through the CM52 column as above, and fractions having $(A_{416}/A_{280})_{ox} = 5.6$ and above were combined and concentrated to 7 mL with 50 mM phosphate buffer at pH 7.0. At this point, the yield was 46 mg and the ratio $(A_{416}/A_{280}) = 5.7$, but SDS–PAGE gel analysis showed the cytochrome b_{562} to be contaminated with ca. 30% impurity proteins of both higher and lower molecular weight. It was further purified by passage through a P30 size exclusion column with 50 mM phosphate buffer at pH 7.4 as column equilibrant and eluent. The cytochrome b_{562} fractions were combined and concentrated to ca. 10 mL. Final yield was ca. 28 mg, $(A_{416}/A_{280})_{ox} = 6.2$. Protein samples for NMR were prepared by solvent exchange with ^2H_2O and concentrated to 4 mM by ultrafiltration in an Amicon cell. The ionic strength of the protein solution was adjusted by the addition of the appropriate amount of either KH_2PO_4 or NaCl, and the pH was adjusted by adding small amounts of 0.2 M ^{2}HCl or NaO^{2}H. The pH was measured on a Beckman Model 3550 pH meter equipped with an Ingold microcombination electrode; cited pH values in ^2H_2O are not corrected for the isotope effect.

The effect of protein concentration was determined on 1.0, 2.0, and 4.0 mM ferricytochrome b_{562} solution in ^2H_2O at 25 °C at the constant buffer concentration of 100 mM phosphate and constant pH 5.46. Ionic strength influences were investigated on a 1.0 mM ferricytochrome b_{562} solution in ^2H_2O at 25 °C by varying the NaCl concentration, 50, 100, and 500 mM, at a constant pH of 5.01; similar spectral changes were observed upon changing phosphate concentration. The pH of a 1.0 mM solution of ferricytochrome b_{562} in 0.5 M NaCl was varied in the limited range from pH 4.5 to 5.6, and spectral properties were found essentially pH independent. The temperature variation on NMR spectral parameters was carried out on a 4 mM protein solution, in 0.8 mM phosphate at pH 4.76. Apocytochrome b_{562} was prepared and purified by the procedure detailed by Warme and Hager (1970). Reconsti-

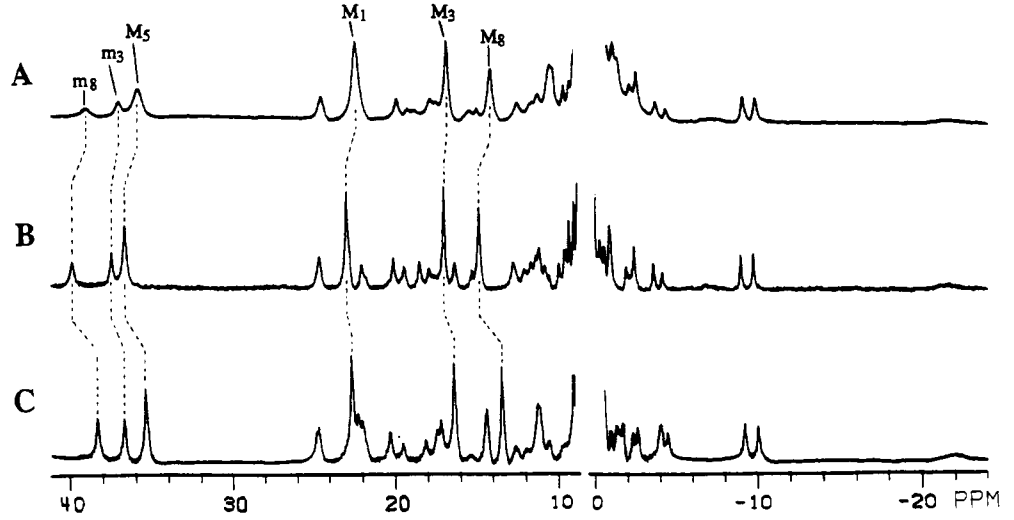

FIGURE 2: Influences of protein concentration and ionic strength on the 500-MHz ^1H NMR spectral parameters of ferricytochrome b_{562} in ^2H_2O at 25 °C at a constant pH of 5.46. (A) 4.0 mM protein in 0.1 M phosphate; this trace closely resembles that reported earlier at lower field (Moore et al., 1985); (B) 1.0 mM protein in 0.1 M phosphate; (C) 4.0 mM protein in 0.8 M phosphate. Note dramatic reduction in line width and small chemical shift changes for peaks labeled m_i, M_i, upon either protein dilution or increased ionic strength.

tution of 5 mg of apoprotein with equimolar amounts of protohemin XIII (Evans, 1977), a hemin with time 2-fold symmetry about the α,γ-meso axis, was monitored optically for the first band, and formation of a folded holoprotein essentially undistinguishable optically from the native protein was confirmed.

NMR Spectroscopy. Ordinary ^1H NMR spectra were recorded on Nicolet NT-500 spectrometers operating at 500 MHz, with spectra recorded in 5 °C intervals over the temperature range 0–65 °C; all spectral changes were completely reversible over this range. Typical spectra resulted from collecting $\sim 10^3$ transients in double precision on 16 384 data points over a 17.5-kHz bandwidth at a repetition rate of 1 s^{-1}. To improve signal-to-noise ratio, the free induction decays were apodized, which introduced 10-Hz line broadening. Chemical shifts for all spectra are referenced to 2,2-dimethyl-2-silapentane-5-sulfonate (DSS) via the residual solvent line. Nonselective T_1 values were determined by the standard inversion–recovery method using a composite 180° pulse; T_1 values for resolved resonances were obtained from the initial slopes of the standard semilogarithmic plots and are accurate to ±10%; for incompletely resolved lines, T_1s were calculated from the delay time which produced a null, τ_{null}, by the relation $T_1 = \tau_{null}/\ln 2$, with uncertainty ±20%. The one-dimensional nuclear Overhauser effect (NOE) measurements were performed at 25 and 35 °C on a 4 mM ferricytochrome b_{562} sample, in 0.8 M phosphate at pH 4.76, by saturating the desired resonance and subtracting from this trace the result of the same experiment with the decoupler placed with an empty spectral region, as described in detail previously (McLachlan et al., 1988).

All two-dimensional ^1H NMR experiments were carried out on a General Electric Ω-500 spectrometer operating at 500 MHz. The spectra were obtained at 25 °C on a 4.0 mM protein solution in 0.8 M phosphate and pH 4.76. The phase-sensitive NOESY spectra were collected with the method as described by States et al. (1982). The conventional N-type COSY spectra were collected with magnitude display (Bax et al., 1981) and are designated as M-COSY hereafter. Solvent suppression, when required, was achieved by direct saturation in the relaxation decay period. A total of 512 blocks were collected with spectral width of 36 363 Hz, and ~128 scans were accumulated for each block with free induction decays of 1024 complex data points. Sixteen dummy scans were used, and a recycle time of 1.6 s, including acquisition, was employed. The 2D data were processed on a μ-VAX II computer with a FORTRAN program FTNMR written by Dr. Dennis Hare. The time domain data were normally multiplied in the $t1$ and $t2$ dimensions by a squared sine bell with phase shifts of 30° for the NOESY spectra and 0° for the M-COSY spectra and were zero-filled to obtain 2K × 2K real data points with a digital resolution of 17.8 Hz/point.

RESULTS

Effect of Solution Conditions. The 500-MHz ^1H NMR spectra of 4 mM ferricytochrome b_{562} in 0.10 M phosphate at pH 5.5 is shown in Figure 2A; the spectral properties compare closely to those reported previously (Moore et al., 1985) except for the improved resolution at the present higher field strength. The line widths of the optimally resolved peaks previously attributed to methyls, labeled M_i, vary from 400 to 100 Hz. Upon simple dilution of the protein to 1 mM at constant temperature, pH, and phosphate concentration, the resulting NMR trace is illustrated in Figure 2B. All resonances, but in particular the peaks marked M_i and m_i, sharpen dramatically and detectably change resonance position. The effect of protein concentration on line widths and shifts for the six resolved methyl resonances (see below) (M_i, m_i) is presented in panels A and B, respectively, of Figure 3. It is clear that both shift and line width approach concentration independence at low ionic strength only at low protein concentration. These changes in line widths and shifts can be taken as direct evidence of aggregation or dimerization of the protein at low ionic strength. Alternatively, the anomalously broadened lines at low ionic strength and high protein concentration (Figure 2A) can be similarly suppressed by markedly increasing the ionic strength, as illustrated by the ^1H NMR trace in Figure 2C, where now fully 40 signals are resolved outside the diamagnetic envelope. A plot of the influence of NaCl concentration on the line width and shift changes of the same six methyl peaks, M_i, m_i, for 1 mM ferricytochrome b_{562} at pH 5.46 and 25 °C is presented in panels C and D, respectively, of Figure 3; both spectral parameters approach constant values only at high NaCl concentration; similar effects were observed for phosphate (not shown). The chemical shifts of the resolved resonances varied inconsequentially in the pH range 4.7–5.5, although all resonances began to change shift and broaden dramatically as the

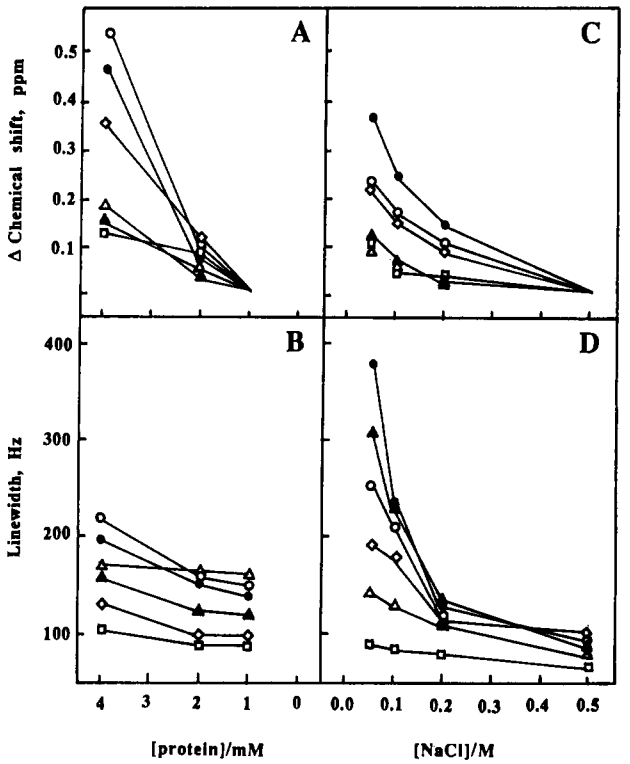

FIGURE 3: Plots of changes in chemical shift, referenced to that observed at 1 mM (A) and observed line width (B) of resolved heme methyl peaks upon increasing the protein concentration from 1.0 to 4.0 mM at 25 °C at invariant pH 5.46 and 0.1 M phosphate concentration. Plots of changes in chemical shifts, referenced to that observed at 0.5 M NaCl (C), and observed line width (D) for the same resonances upon decreasing the ionic strength from 0.5 to 0.05 M NaCl at 25 °C at constant pH 5.46 and 4 mM protein concentration. Note the similar suppression of anomalous line broadening at both low protein concentration and high ionic strength. Symbols: (●) m_8; (▲) m_3; (○) M_5; (△) M_1; (□) M_3; (◇) M_8.

pH is raised above 6, as discussed previously (Moore et al., 1985). We focus further studies solely on the low-pH form near pH 5. The optimally resolved ^{1}H NMR trace of a 4 mM protein at 25 °C, pH 4.76, is illustrated in Figure 4, where all resonances are labeled, and serves as the reference base for the 2D NMR spectra; the chemical shifts are listed in Table I. Direct determination of nonselective T_1 values for resolved resonances by the inversion–recovery technique yielded the values included in Table I.

The spectrum in Figure 4 also provides direct evidence for protein structural and/or conformational heterogeneity, in that resonance intensities vary over a ratio of 6:3:2:1 (i.e., peaks labeled M_5, m_8, H_6, and h_7 in Figure 4). This is further supported by the fact that the number of well-resolved resonances (~41) greatly exceeds that observed for any homogeneous low-spin ferric hemoprotein (Satterlee, 1985). Systematic analysis of peak areas as a function of solution conditions allows us to factor all resonances as belonging to two sets, M_i, H_i and m_i, h_i, with a constant M_i:H_i and m_i:h_i ratio of 3:1, reflecting likely methyls and single proton for each species, and the ratio of M_i:m_i or H_i:h_i ~2:1 for the two molecular entities. Reconstitution of apocytochrome b_{562} with the symmetric hemin, protohemin XIII, yielded a spectrum very similar to that of the native protein, but with only about half the number of resolved resonances (not shown); the low-field heme methyl resonances appeared at 18.0, 18.3, 38.6, and 40.3 ppm; the low-field single proton signals, at 11.5, 12.4, 12.7, 13.7, 18.6, 19.7, 19.9, 22.1, and 25.1 ppm.

Assignment of Hyperfine-Shifted Peaks. The 2D NMR data were collected at 25 °C, pH 4.76, which provided the optimal resolution; the reference trace is shown in Figure 4. The split diagonal portions of magnitude COSY (A) and NOESY (B and C) maps for the hyperfine-shifted peaks are illustrated in Figure 5. An expanded region 2.5 to −4.5 ppm is shown in Figure 6. For the major isomer (cross peaks connected by solid lines), COSY peaks characteristically identify two vinyl groups, peaks H_2, $H_{2'}$, $H_{2''}$ and H_4, $H_{4'}$, $H_{4''}$, as confirmed by parallel NOESY peaks. One propionate group, peaks H_6, $H_{6'}$, $H_{6''}$, $H_{6'''}$, is easily identified in the COSY

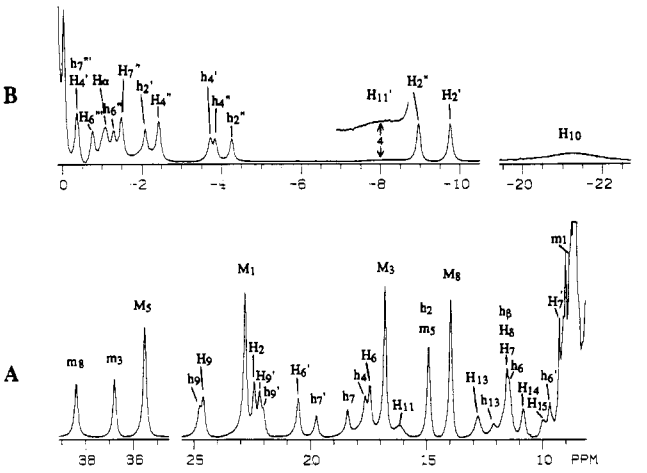

FIGURE 4: Optimally resolved 500-MHz ^{1}H NMR traces for the low-field (A) and upfield (B) hyperfine-shifted region of 4.0 mM ferricytochrome b_{562} in ^2H_2O, pH 4.75, 0.8 M phosphate. This trace serves as the reference for the 2D map. The resonance labels are M_i, m_i for methyls and H_i, h_i for single protons with M_i, H_i and m_i, h_i originating from the major and minor isomeric forms in solution. The subscript reflect the assignments as listed in Table I.

Table I: Proton Chemical Shift and T_1s of 4 mM Ferricytochrome b_{562} in ^2H_2O and 0.8 M Phosphate, pH 4.76 at 25 °C

		major isomer		minor isomer	
label χ_i[a]	assignment	shift (ppm)[b]	T_1 × 10 (ms)	shift (ppm)[b]	T_1 × 10 (ms)
1	1-CH_3	22.70	6.4	8.72	
2	2-H_α	22.35	5.1	14.21	8.2
2′	2-$H_{\beta c}$	−9.80	11	−1.95	13
2″	2-$H_{\beta t}$	−8.99	10	−4.21	10
3	3-CH_3	16.46	7.8	36.79	4.2
4	4-H_α	8.56	8.7	17.55	4.3
4′	4-$H_{\beta c}$	−0.36	14	−3.74	8.7
4″	4-$H_{\beta t}$	−2.41	12	−3.87	11
5	5-CH_3	35.42	4.4	14.21	5.9
6	6-H_α	17.28	5.8	11.35	2.2
6′	6-$H_{\alpha'}$	20.44	5.1	9.88	6.5
6″	6-H_β	1.92	5.8	−1.27	
6‴	6-$H_{\beta'}$	−0.78		0.24	5.8
7	7-H_α	11.50	6.1	18.23	4.9
7′	7-$H_{\alpha'}$	9.21		19.66	
7″	7-H_β	−1.50	6.5	2.00	
7‴	7-$H_{\beta'}$	0.13	22	−0.36	3.2
8	8-CH_3	13.55	9.4	38.29	
α	α-meso-H	−1.12	1.6		
δ	δ-meso-H	11.5	2.5		
β	β-meso-H			11.50	2.5
9	His-102 $C_\beta H$	24.75	2.7	24.89	2.7
9′	His-102 $C_\beta H'$	22.10	2.5	22.02	
10	His-102 ring CH	−21.2	<0.2		
11	Met-7 $C_\gamma H$	16.2	<0.4		
11′	Met-7 $C_\gamma H'$	−8.3	<0.2		
12	Met-7 $C_\epsilon H_3$	4.0[c]			
13	*d*	12.8	0.9	12.2	0.7
14	*d*	10.77	1.4		
15	*d*	9.96	2.2		

[a] Subscripts in peak labels (M_i,m_i) or (H_i,h_i). [b] Referenced to DSS. [c] Shift interpolated via the Curie plot in Figure 8C. [d] Not assigned.

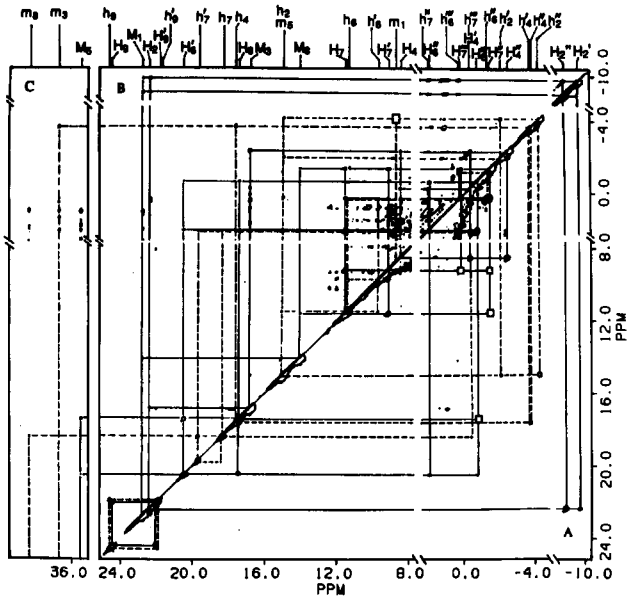

FIGURE 5: Split diagonal section of the magnitude COSY (A) and NOESY (B, C) maps at 500 MHz for 4 mM ferricytochrome b_{562} in ^2H_2O and 0.8 mM phosphate at pH 4.75; only the regions relevant to assigning the resolved heme resonances are shown. The spin connectivities that allow all assignments are indicated in solid and dotted lines for the major and minor isomers, respectively. The assignmed resonances are indicated along the $t2$ dimensions at the top of the figure. The small squares indicate weak cross peaks observed only at lower contour levels.

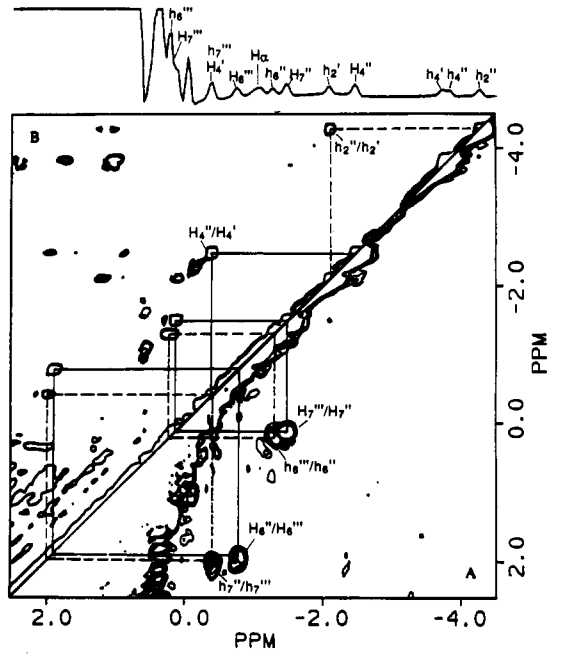

FIGURE 6: Expanded upfield split diagonal section of the same magnitude COSY (A) and NOESY (B) maps shown in Figure 5, which provide the needed spin connectivity for identifying the vinyl and propionate β-protons. Major and minor isomer connectivities are marked by solid and dotted lines, respectively.

map and confirmed by the expected NOESY peaks. Three additional pairs of strongly coupled proton pairs, (H_7, $H_{7'}$), ($H_{7''}$, $H_{7'''}$), and (H_9, $H_{9'}$), are located in the COSY map, and the pairwise NOESY peaks between the sets identify the former two pair as arising from the second propionate. Having identified all spin-coupled protons for the heme, we conclude that the pair H_9, $H_{9'}$ must arise from an amino acid side chain. The NOESY peak between the apparent methyl peaks, M_i and the above-identified vinyl or propionate groups, allows individual assignment of all groups (Keller & Wüthrich, 1981; McLachlan et al., 1988). Thus NOESY peaks between the vinyl peaks $H_{2'}$, $H_{2''}$ and M_1, and between $H_{4'}$, $H_{4''}$, and M_3, locate the methyls adjacent to vinyls, and the NOESY peaks between M_5 and H_6, $H_{6'}$ and between M_8 and H_7, $H_{7''}$, locate the methyls on the propionate-bearing pyrroles. Distinction between the two methyls of each type is made on the basis of the NOESY cross peak between M_1 and M_8, which identifies them uniquely as 1-CH_3 and 8-CH_3 and dictates that the subscripts on the resonances correctly identify the position of the substituent on the heme in each case, as shown in Figure 1. The assignments and chemical shifts are listed in Table I.

Assignments for the minor isomer peaks proceed in a parallel manner, although with a less complete set of cross peaks. The characteristic COSY cross peaks uniquely locate the vinyls again, h_2, $h_{2'}$, $h_{2''}$ and h_4, $h_{4'}$, $h_{4''}$. Five sets of strongly coupled proton pairs are seen in the COSY map, (h_9, $h_{9'}$), (h_6, $h_{6'}$), ($h_{6''}$, $h_{6'''}$), (h_7, $h_{7'}$), and ($h_{7''}$, $h_{7'''}$). Both COSY and NOESY cross peaks identify (h_7, $h_{7'}$) and ($h_{7''}$, $h_{7''}$) from one propionate group and (h_6, $h_{6'}$) and ($h_{6''}$, $h_{6'''}$) from the other propionate. The proton set (h_9, $h_{9'}$) does not arise from a propionate and hence must originate from an amino acid side chain. The NOESY map again identifies methyl peaks m_5 and m_8 as located adjacent to propionates and m_3 as adjacent to a vinyl group (Figure 5). The fourth methyl, m_1, incompletely resolved on the shoulder of the aromatic region, also yields a NOESY peak to a vinyl proton $h_{2''}$. Unlike the case of the major isomer, the NOESY map had insufficient sensitivity to detect the inter-methyl NOE to uniquely identify all substituents. However, the improved sensitivity of ordinary 1D NOE indicated a weak NOE between m_8 and m_1 (not shown), leading to the assignments listed in Table I, with the peak subscript i = 1–8 reflecting the substituent position on the heme in the Fischer notation.

NOESY peaks locating meso-H resonances could not be identified, likely due to the much weaker NOEs expected for the much faster relaxing meso-H resonances. Previous ^1H NMR titrations of ferrocytochrome b_{562} with ferricytochrome b_{562} had indicated that one meso-H of the former is shifted a few ppm to low field upon oxidation (Moore et al., 1985). Partial saturation of the remaining unassigned resolved single-proton resonances failed to yield detectable resonances except for the broad peak under H_7, h_6 (not shown). However, 1D NOE studies at 35 °C, where the resonances H_δ and h_β are resolved (Figure 7D), reveal dipolar connectivity between H_δ and M_1 (1-CH_3) and M_8 (8-CH_3), and between h_β and m_5 (5-CH_3) and h_4 (4-H_α), establishing that they are meso-H resonances for the δ- and β-position of the major and minor isomers, respectively. Similarly, the upfield rapidly relaxing peak H_α yields NOEs to H_2 (2-H_α) and M_3 (3-CH_3), indicating it arises from the α-meso-H of the major isomer (not shown; see supplementary material).

The geminal nature of peak H_9, $H_{9'}$ (and h_9, $h_{9'}$), as evidenced by intense COSY and NOESY cross peaks, together with their hyperfine shifts and T_1 values, strongly supports their origin as the axial His-102 C_βHs: ferricytochrome c and b_5 exhibit similar shifts and T_1s for peaks assigned to the axial His C_βHs (Moore & Williams, 1984; McLachlan et al., 1988). One of the two upfield broad single proton peaks, likely H_{10}, must also originate from one of the His-102 ring CHs, as found in both ferricytochrome c and b_5. The usual strongly upfield-shifted C_γHs and $C_\epsilon H_3$ characteristic of coordinated Met in low-spin ferricytochromes c (Satterlee, 1985) are not observed at 25 °C. However, evidence for such peaks is found

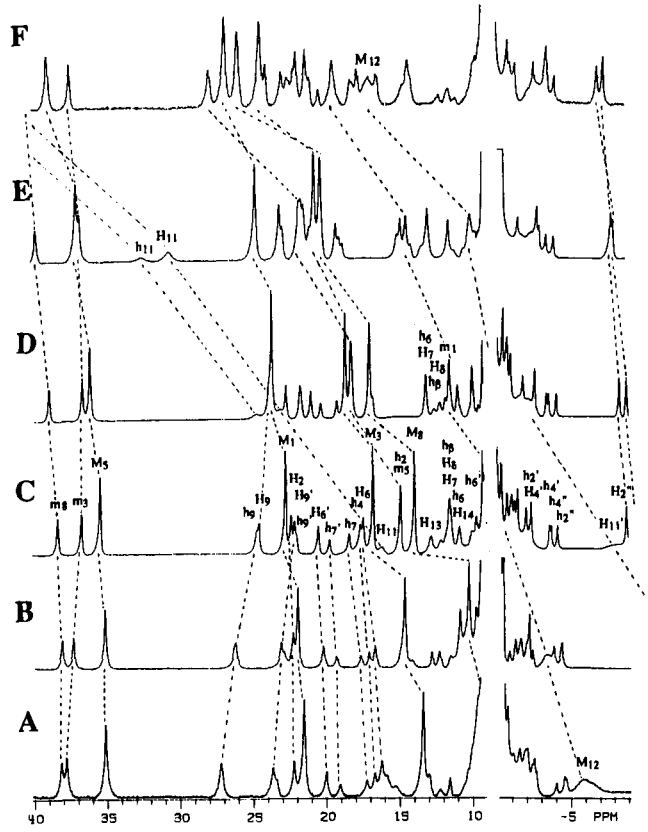

FIGURE 7: Resolved portion of the 500-MHz ^{1}H NMR spectra of 4.0 mM ferricytochrome b_{562} in ^2H_2O and 0.8 mM phosphate over the temperature range 0–60 °C: (A) 0 °C, (B) 10 °C, (C) 25 °C, (D) 35 °C, (E) 45 °C, and (F) 60 °C. The dotted lines follow the temperature profiles of peaks particularly relevant to determining the molecular nature of the high-spin species populated at elevated temperature. The labeling of resonances is the same as that given in Table I and Figure 4.

at other temperatures (see below).

Temperature Dependence. The hyperfine shifts and line widths displayed rather remarkable behavior when compared to the well-characterized ferricytochromes *c* and b_5, as shown in a set of variable-temperature traces in Figure 7 and the Curie plots for the individual resonances in Figure 8. Instead of hyperfine shifts decreasing at elevated temperatures, as expected by the Curie law (Jesson, 1973), the majority of the resonances displayed increased shifts at higher temperatures. The temperature profiles of the various resonances in Figure 8 can be placed into three broad categories: Curie-like, with the shifts decreasing with increasing temperature in a manner generally found for ferricytochromes *c* [the His 102 $C_\beta H$ peaks (H_9, $H_{9'}$) and (h_9, $h_{9'}$), peaks H_{13}–H_{15}; Figure 8A,B); anti-Curie, where the shifts increase rather than decrease with increasing temperature (all heme methyls, propionate H_αs, vinyl H_αs, and most H_βs for both substituents; Figure 8A,B); and peaks with such dramatic deviations that the hyperfine shift either changes sign or extrapolates to such a change of sign over the detected temperature range (note in particular the peaks H_{11}, $H_{11'}$, M_{12}; Figure 8C).

The prominent three-proton broad resonance M_{12} appears on the upfield site of the diamagnetic envelope only at the lowest temperature (0–10 °C; i.e., Figure 7A,B) and must arise from a rapidly relaxing methyl in addition to those from the heme, i.e., the likely Met-7 $C_\epsilon H_3$ (Wüthrich, 1970). A similarly strongly relaxed apparent methyl peak is resolved from the diamagnetic envelope on the low-field side above 50 °C (Figure 7D,E). The Curie plots for the two peaks fall on the same line (M_{12} in Figure 8C) and hence can be concluded to originate from the same methyl group, Met-7 $C_\epsilon H_3$. Hence the Met-7 methyl approaches its upfield shifts characteristic of low-spin ferricytochromes only at very low temperature.

It is noted that the only resolved peaks attributed to meso-Hs, H_α, H_δ, and h_β, move sharply downfield with increasing temperature, while the remainder of the unassigned low-field peaks, H_{13}, h_{13}, H_{14}, and H_{15}, show Curie-like behavior (Figure 8A). Moreover, numerous other single-proton resonances exhibit anti-Curie behavior and move downfield out of the diamagnetic only at elevated temperature (Figure 7D,E); degraded resolution due to heme disorder and increased line width at the elevated temperatures precluded identifying these peaks at this time.

Discussion

Protein Aggregation. The influence of protein concentration on NMR spectral parameters, as reflected in the two traces in Figure 2A,B and the plots in Figures 3A,B, gives direct evidence for aggregation at low ionic strength. A very similar change in spectral parameters is induced at fixed protein concentration upon dramatically increasing ionic strength, as shown in Figure 3C,D. It is noted, however, that the effects of protein concentration and ionic strength are not uniform on the various resonances and are, in fact, highly selective. Thus, the most dramatic changes in shifts and line widths that accompany aggregation occur for 5-CH_3 and 8-CH_3 in both isomer forms in solution, and for the 6-H_αs of the major isomer. These are the methyls on the two pyrroles exposed to solvent (Mathews et al., 1979), and hence this argues that the interprotein interaction is likely very stereospecific, since the selective influence on the heme must represent localized perturbations, probably involving changes in the rotational positions of the heme propionates.

It has been noted that ferricytochrome b_{562} in the crystal forms tight intermolecular contacts between the two molecules of the unit cell and that these contacts are across the heme binding site near the axial His-102, involving a pair of symmetrical interactions of Arg-98 and His-102 of one molecule interacting with Gln-103 of the other molecule (Mathews et al., 1979; Moore et al., 1985). It is therefore likely that the same "dimer" interaction occurs in solution and accounts for the concentration/ionic strength effects observed. Strong ionic strength effects on the CD spectra of both ferri- and ferrocytochrome b_{562} have been reported by Meyer and Bullock (1978) and were attributed to ionic strength perturbations of surface side-chain orientations; protein concentration influences were not investigated in that study. The present ^{1}H NMR data confirm the importance of high ionic strength to give spectral parameters independent of solution conditions but show that the ionic strength influence involves both the breakup of aggregates and a likely reorientation of surface side chains. The earlier observation of strong ionic strength effects on the reduced protein as well (Myer & Bullock, 1978) suggests that both forms of the protein may aggregate in a similar fashion. Such interaction across the heme surface between oxidized and reduced proteins may account for the unusually rapid electron self-exchange reported previously (Moore et al., 1985). For the present purposes, we restrict all further interpretation of ^{1}H NMR spectral parameters to conditions where the protein appears monodisperse, i.e., at ~0.8 M phosphate, which affords the optimally resolved ^{1}H NMR spectrum.

Structural Basis of Heterogeneity. The above resonance assignments at 25 °C establish the presence of two isomers in solution in the ratio ~2:1. The pattern of hemin hyperfine shifts at 25 °C for the two isomers is very similar, typical of

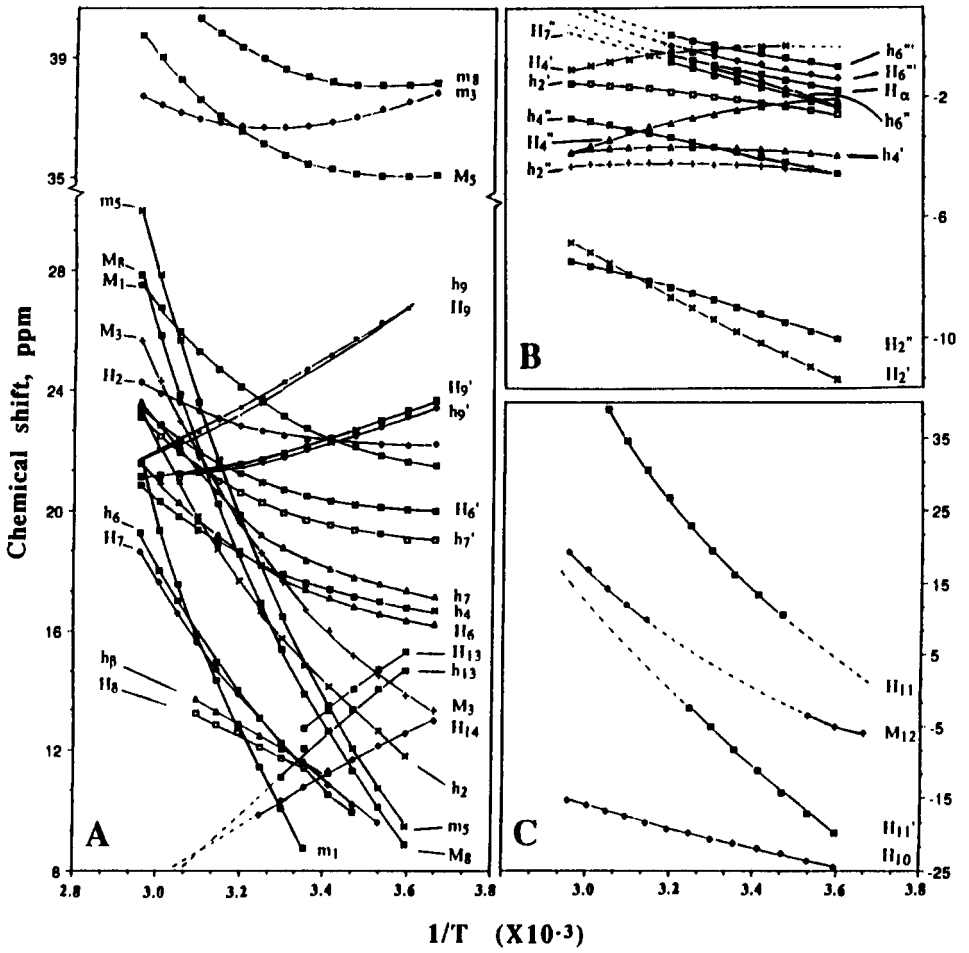

FIGURE 8: Plots of observed chemical shifts relative to DSS versus reciprocal absolute temperature (Curie plot) of 4.0 mM ferricytochrome b_{562} in ^2H_2O and 0.8 mM phosphate, pH 4.75, for the resolved low field (A) and upfield (B). Section C is the Curie plot for the strongly relaxed signals. M_{12} appears only at low and high temperature. The Curie plot (C) finds M_{12} on the same line, and hence the upfield signal at 0 °C must be the same as the low-field signal at 60 °C, i.e., the Met-7 $C_\epsilon H_3$; note the considerably compressed chemical shift scale in (C) relative to (A) and (B). The two broad lines H_{11}, $H_{11'}$ exhibit similarly dramatic temperature profiles which, like M_{12}, extrapolate to upfield contact shifts at low temperature and low-field contact shifts at high temperature and are assigned to Met-7 $C_\gamma Hs$.

a primarily low-spin ferric hemoprotein, with many lines for the two isomers appearing as pairs with similar shifts. The hyperfine shift pattern for the two isomers, however, differs in the pattern of unpaired spin density, where the largest π spin density is on pyrrole I (1-CH_3, 2-H_α) and III (5-CH_3, 6-H_αs) in the major form, but on pyrrole II (3-CH_3, 4-H_α) and pyrrole IV (8-CH_3, 7-H_αs) in the minor isomer. Moreover, the single downfield meso-H is δ-meso-H for the major and β-meso-H for the minor isomer. This is the same difference in hyperfine shift patterns for the two isomers found in, for example, ferricytochrome b_5 (McLachlan et al., 1988) and certain cyano complexes of ferric myoglobin and hemoglobin (Lecomte et al., 1985; La Mar et al., 1985), which could be uniquely traced to heme orientations differing by a 180° rotation about the hemin α,γ-meso axis (Figure 1A,B). It has been demonstrated in ferricytochromes *c*, however, where the heme is covalently bound to the protein matrix, that a similar two sets of hyperfine-shifted hemin resonances reflecting 90° rotation of the orbital hole can occur solely due to the alternate chiralities that can be adopted by the axial Met (Figure 1A,C) (Senn et al., 1980; Senn & Wüthrich, 1983b, 1985). Hence the presently observed heterogeneity could arise from either heme orientational disorder or disorder in the chirality of the axial iron–Met-7 bond.

The detailed hyperfine shift patterns for the individual isomers indicate similar contact shifts for 5-CH_3 and 8-CH_3 (because of pseudo-2-fold symmetry) and a difference in 1-CH_3 and 3-CH_3 shifts (nonsymmetrically paired) which is essentially the same as for ferricytochrome b_5 (La Mar et al., 1981), where heme orientational disorder could be unequivocally established. With the limited hemin available, a single reconstitution with a 2-fold symmetric hemin (protohemin XIII) afforded a homogeneous sample with only half the resolved ^1H NMR resonances of the native protein (not shown), directly supporting heme orientational disorder as the sole origin of the heterogeneity. An insufficient number of noncoordinated amino acid signals have been assigned to date to unequivocally establish whether the two sets of peaks do or do not exhibit the same dipolar contacts with the protein matrix. Preliminary data suggest that substituents of pyrrole II of the major isomer yield NOEs to peaks in the aromatic envelope (not shown), as expected on the basis of the crystal structure. However, a definitive determination must await futher amino acid signal assignments.

Axial Ligands. The geminal nature of the proton sets H_9, $H_{9'}$ or h_9, $h_{9'}$ is established by the COSY cross peaks and intense NOESY peaks for their relatively short T_1s (Table I). They likely constitute the $C_\beta Hs$ of axial His-102 for each isomer, since the shifts and relaxation properties are very similar to those found for known His $C_\beta Hs$ in other low-spin ferric hemoproteins (Moore & Williams, 1984; McLachlan et al., 1988; Thanabal et al., 1988; Emerson & La Mar, 1990a). The larger downfield bias for the mean $C_\beta H_2$ hyperfine shift in ferricytochrome b_{562} is consistent with sig-

nificant hydrogen-bond donor character of the His-102 ring (Thanabal et al., 1988). The conversion of the acidic to the alkaline form has been proposed to involve primarily the abstraction of the His-102 ring proton to yield an axial imidazolate (Moore et al., 1985), as also observed for the structurally related ferricytochromes c' (Weber, 1982; Jackson et al., 1983). The strong upfield bias of peak H_{10}, the likely His-102 $C_\epsilon H$, as compared to other ferricytochromes c and b_5, also supports H-bond donation by the His-102 ring NH (Chacko & La Mar, 1982; Thanabal et al., 1988).

Conspicuous by their absence in the 25 °C ^{1}H NMR trace for ferricytochrome b_{562} are the strongly relaxed and upfield-shifted methyl and single-proton peaks characteristic of axial Met bonding, as found in the overwhelming majority of low-spin ferricytochromes c (Satterlee, 1985; Senn & Wüthrich, 1983a–c, 1988; Senn et al., 1980, 1983, 1984b; Moore & Williams, 1977). The prominent Met methyl resonance is found with variable upfield bias in numerous ferricytochromes c and has been proposed to reflect the strength of the axial iron–Met bond, which in turn may contribute to modulating redox potential (Moore & Williams, 1977). In the present ferricytochrome b_{562}, such an upfield-shifted methyl peak (M_{12}) appears only at very low temperature (Figure 7A,B), and the efficient relaxation clearly dictates that it must arise from the axial Met-7. The unusual shift of the proposed Met-7 $C_\epsilon H_3$ resonance position is suggestive of a perturbed bond, and evidence for such a perturbation is found in the temperature dependence of the hyperfine-shifted resonances (see below).

Heme Electronic Structure. At the lowest accessible temperature, the hyperfine shift pattern for both hemin and the axial His and Met are typical of low-spin ferric hemins (La Mar, 1979; Satterlee, 1985), as found in the mitochondrial or bacterial ferricytochromes c with the same ligation (Senn & Wüthrich, 1985). The hyperfine shift pattern for the hemin, as reflected characteristically by the four methyls, is highly asymmetric and is determined primarily by the contact interaction. The unpaired spin density pattern, which reflects the orbital hole in low-spin ferric hemins, has been demonstrated to be controlled either by the orientation of the axial His imidazole plane (Shulman et al., 1971; Emerson & La Mar, 1990b) or by the axial Met chirality (Senn et al., 1980; Senn & Wüthrich, 1983b,c). In ferricytochromes c, the axial His is generally oriented parallel to a meso–iron–meso axis, so that the orbital hole is controlled by the Met chirality (Senn & Wüthrich, 1985). The contact shift pattern or asymmetric spin delocalization in ferricytochrome b_{562} has the lone spin largely restricted to the trans pyrroles I and III in the major isomer. Inspection of the crystal coordinates (Mathews et al., 1979) reveals that both the His orientation and Met bonding are so as to predict the same unpaired spin asymmetry (Figure 1A), namely, that observed experimentally. Therefore, the contact shift pattern does not allow us to ascertain the relative importance of the two axial bonds in controlling the orbital ground state in ferricytochrome b_{562}.

In contrast to observations on numerous ferricytochromes c and b_5, as well as other low-spin ferric hemoproteins, where the majority of the hyperfine-shifted resonances essentially follow the Curie law, i.e., hyperfine shifts decrease as the temperature is raised, the majority of the peaks for ferricytochrome b_{562} exhibit anti-Curie behavior (Figures 7 and 8). In fact, all resonances assigned to heme pyrrole α-substituents exhibit anti-Curie behavior. For the proposed axial His-102 peaks, the $C_\beta Hs$ [(H_9, $H_{9'}$), (h_9, $h_{9'}$)] exhibit more normal Curie behavior, while the proposed ring CH (H_{10}) actually decreases in shift with increasing temperature faster than T^{-1}. The methyl peak M_{12} assigned to the axial Met-7 $C_\epsilon H_3$, as well as the two single-proton peaks, H_{11} and $H_{11'}$ (and h_{11}), on the other hand, exhibits not only extraordinary strong downfield shifts on increasing temperature, but the contact shift direction changes sign, i.e., all three will directly exhibit either upfield (low T) or downfield (high T) contact shifts (peak M_{12}) or have temperature dependence that extrapolates to such changes in the sign of the shift (H_{11}, $H_{11'}$) (Figure 8C).

Ferric hemoproteins in a given spin ground state invariably exhibit Curie-like behavior for the majority of hyperfine-shifted resonances (Jesson, 1973; Satterlee, 1985), and strong and systematic deviations from Curie behavior are generally taken as direct evidence for a spin-state equilibrium (Iizuka & Morishima, 1974). The present observation of anti-Curie behavior for the hemin methyls, together with their low-temperature shifts, clearly dictates the presence of a low-spin ($S = {}^1/_2$) ground state in rapid equilibrium with a thermally accessible high-spin ($S = {}^5/_2$) state. The nature of the deviations from Curie behavior for different resonances in such an equilibrium depends on their relative shift differences in the low-spin, $S = {}^1/_2$, and high-spin, $S = {}^5/_2$, states. Thus functional groups that exhibit the same direction and similar shift magnitude in high-spin and low-spin states should exhibit near-Curie behavior in spite of the spin equilibrium. Protons with larger shifts of the same direction in high-spin than in low-spin form would exhibit anti-Curie behavior because of the larger effect of populating the high-spin state than the T^{-1} change of the low-spin state. On the other hand, protons with hyperfine shifts in different directions in the low-spin and high-spin states would, on the same basis as above, necessarily show Curie-like behavior, but with a much steeper slope than T^{-1} and a strong possibility that the observed contact shift actually changes sign over the accessible temperature range.

Two possibilities for the high-spin state must be considered, a six-coordinate state where the spin equilibrium is within an invariant ligation state [such as for an intermediate ligand field observed for methydroxy- or metazidomyoglobin (Antonini & Brunori, 1971)] or a five-coordinate state where one ligand–iron bond ruptured. The largely contact shift patterns for both hemin and axial His in high-spin ferric hemoproteins are highly characteristic of the ligation state, differing primarily in the meso-H shift direction (La Mar & Walker, 1978; La Mar, 1979). Representative shift values for the different resonance, taken from *Aplysia* metmyoglobin or *Rhodopseudomonas palustris* ferricytochrome c' (Jackson et al., 1983; Pande et al., 1986) for five-coordinate, and sperm whale metaquomyoglobin (La Mar et al., 1980) for six-coordinate species, are listed in Table II, where they are compared to the shifts of low-spin ferricytochrome with His/Met ligation. It is clear from inspection of Table II that increased population of either a five- or six-coordinate high-spin form at elevated temperatures would result in anti-Curie behavior for heme methyls, propionate H_α and vinyl H_α resonances. Similarly, the shift for His in Table II predicts Curie-like behavior for $C_\beta Hs$. Thus the observed deviations (or lack thereof) from the Curie law for pyrrole substituents and the axial His resonances are completely consistent with the proposed spin equilibrium without discriminating between the alternate ligation states of the high-spin species. The meso-H shifts, however, allow a distinction to be made, since, for a six-coordinate high-spin form, the observed shifts in the presence of the spin equilibrium should be anti-Curie (like heme methyls[2]), while a five-coordinate high-spin state would predict

Table II: Characteristic Hemin and Axial His Hyperfine Shifts in Low-Spin and High-Spin Ferric Hemoproteins[a]

		high spin	
	low spin[b]	five coordinate[c]	six coordinate[d]
heme			
methyls	~20	~70	~75
vinyl H_α	~15	~40	~40
vinyl H_β	~-5	~-5	~-5
propionate H_α	~15		
meso-Hs	~5	~-40	~+40
His			
$C_\beta Hs$	15	15	15
ring $C_\epsilon H$	-5 to -10	low field	low field
ring $C_\delta H$	15-20	low field	low field

[a] Shifts in ppm from DSS, in ^2H_2O at 25 °C. [b] Mean shifts at 25 °C for cytochrome b_{562}, although essentially the same as for ferricytochrome b_5 or ferricytochrome *c*. [c] Shifts taken from Pande et al. (1986) and Jackson et al. (1983). [d] Data taken from La Mar et al. (1980).

steeper temperature slope than T^{-1}. The assigned meso-Hs for each isomer (H_α, H_δ, h_β) clearly move strongly downfield at higher temperature (Figure 8A,B), dictating that the high-spin species is six-coordinate, i.e., the His/Met ligation remains intact. The other unassigned single proton resonances that become resolved in the low-field region at >45° are likely the remaining meso-Hs which resonate under the diamagnetic envelope in the low-spin state. The unassigned resonances which exhibit Curie-like behavior, H_{13}, H_{14}, and H_{15}, likely arise from noncoordinate heme pocket residues which exhibit dipolar shifts characteristic solely from the low-spin state (La Mar, 1979; Satterlee, 1985; Emerson & La Mar, 1990a).

The nature of the temperature profile of the Met-7 $C_\epsilon H_3$ peak (M_{12}) directly supports the maintenance of the iron–Met bond in the high-spin state and provides indirect information on the nature of the contact shifts pattern for an axial Met in a high-spin system. Thus the change in sign from upfield to low field for the $C_\epsilon H_3$ (M_{12}) signal demands that Met-7 experiences large contact shifts in both spin states, upfield in the low-spin (as in ferricytochromes *c*) and large downfield contact shifts in the high-spin form at elevated temperatures. Moreover, the two major isomer single-proton peaks, H_{11}, $H_{11'}$, display temperature profiles very similar to that of Met-7 $C_\epsilon H_3$ signal M_{12}, in that they extrapolate to changes in sign from upfield at low temperature to strongly downfield at high temperature (Figure 8C). This is precisely what would be expected for the two Met-7 $C_\gamma Hs$, which sould experience contact shifts similar to the $C_\epsilon H_3$ in both states (Wüthrich, 1969). Hence we assign H_{11}, $H_{11'}$ to the two Met-7 $C_\gamma Hs$. From these latter results we further draw the conclusion that the contact shift pattern for a high-spin iron(III) bound Met has large low-field $C_\epsilon H_3$ and $C_\gamma H$ contact shifts, consistent with the expected dominant σ spin delocalization (La Mar & Walker, 1978; La Mar, 1979). On the basis of the fractional high-spin population of ~12% at 45 °C which is derived from the mean heme methyl shifts,[3] we estimate that the pure high-spin contact shifts for a bound Met $C_\epsilon H_3$ (M_{12}) is ~270 ppm and $C_\gamma H$ (H_{11}) ~470 ppm.

Low-spin ⇄ high-spin equilibria for ferric hemoproteins are not uncommon (Antonini & Brunori, 1971), although only infrequently observed among other cytochromes with axial His/Met ligation. Previously reported NMR spectra of structurally characterized ferricytochromes with His/Met ligation exhibit temperature-dependent shifts indicative of a low-spin ferric state (Wüthrich, 1970). There are several examples of structurally less characterized ferricytochromes *c* which exhibit similar spin equilibria (Hon-Nami et al., 1980; Timkovich & Cork, 1984; Timkovich et al., 1984; Saraiva et al., 1990). The thermally accessible six-coordinate high-spin state in ferricytochrome b_{562} is in contrast to the behavior observed for the majority of ferricytochromes *c* and demands that the effective axial field (i.e., either the His–Fe and/or Fe–Met bond) is weakened in the present protein. The ^1H NMR data only dictate that both His and Met are ligated and hence do not indicate which is perturbed relative to that in the ferricytochromes *c*. It has been noted, however, that the characteristic "695"-nm band of ferricytochromes *c*, assigned to a Met → Fe charge-transfer band (Dickerson & Timkovich, 1975), is found at 720 nm in ferricytochrome b_{562} (Myer & Bullock, 1978; Moore et al., 1985), indicating that the iron–Met bond must be perturbed.

The mean heme methyl chemical shifts at 45 °C for the major and minor isomer are 25.6 and 28.2 ppm, respectively; this suggests that the minor isomer exhibits a larger high-spin population (La Mar et al., 1983). The proposed Met-7 $C_\gamma H$ peak similarly exhibits a larger shift at 45 °C for the minor (h_{11} ~ 32.6 ppm) than major (H_{11} ~ 30.7 ppm) isomer. This suggests coupling of the equatorial heme–protein contacts to the axial position so that the minor component hemin orientation results in a slightly weaker axial field than in the major isomer. Current efforts are centered on detailed 2D NMR analysis of the heme pocket structure of ferricytochrome b_{562} reconstituted with symmetric hemins that yield both significantly improved resolution and sensitivity for the homogeneous protein and should allow assignment for all Met-7 signals and identification for the titrating groups modulating the redox potential (Moore et al., 1985).

Acknowledgments

We are indebted to K. Rajarathnam for experimental assistance and to Professor Kevin M. Smith for a gift of protohemin XIII.

Supplementary Material Available

Reference traces (35 °C) of ferricytochromes b_{562} and the 1D NOE differences traces identifying the meso-H resonances (one figure) and slices of the 2D COSY and NOESY map identifying the connectivity for the major component heme resonances (three figures) (4 pages). Ordering information is given on any current masthead page.

References

Ames, G. F.-L., Prody, C., & Kustu, S. (1984) *J. Bacteriol. 160*, 1181–1183.

Antonini, E., & Brunori, M. (1971) *Hemoglobin and Myoglobin and Their Reactions with Ligands*, pp 40–54, North-Holland Publishing Co., Amsterdam.

Bax, A., Freeman, R., & Morris, G. (1981) *J. Magn. Reson. 42*, 164–168.

Bullock, P. A., & Myer, Y. P. (1978) *Biochemistry 17*, 3084–3091.

[2] The dramatic difference in the deviations from the Curie law for the four methyls is due to the fact that they possess very similar contact shifts in the high-spin form but very different contact shifts in the low-spin species. Thus the degree of deviation increases $M_5 < M_1$ $M_3 < M_8$, which parallels the decrease in contact shifts for the low-spin form.

[3] Using the mean methyl shift ~28 ppm observed at 45 °C, as compared to that expected for pure low spin (22 ppm) or pure high spin (72 ppm) at the same temperature, we estimate 12% high-spin character. Taking the pure low-spin Met $C_\epsilon H_3$ and $C_\gamma H$ shift at -25 and -30 ppm, the observed shifts of 10 and 30 ppm translate to 270 and 470 ppm shifts for those groups for a pure high-spin state.

Chacko, V. P., & La Mar, G. N. (1982) *J. Am. Chem. Soc., 104*, 7002–7007.
Dickerson, R. E., & Timkovich, R. (1975) in *The Enzymes* (Boyer, P., Ed.) 3rd ed., Vol. 11, pp 397–547, Academic Press, New York.
Emerson, S. D., & La Mar, G. N. (1990a) *Biochemistry 29*, 1545–1555.
Emerson, S. D., & La Mar, G. N. (1990b) *Biochemistry 29*, 1556–1566.
Evans, B. (1977) Ph.D. Thesis, University of Liverpool.
Ghelis, C., & Yon, J. (1982) *Protein Folding*, pp 374–418, Academic Press, New York.
Hager, L. P., & Itagaki, E. (1967) *Methods Enzymol. 10*, 373–378.
Hon-Nami, K., Kihara, H., Kitagawa, T., Mijazawa, T., & Oshima, T. (1980) *Eur. J. Biochem. 110*, 217–223.
Iizuka, T., & Morishima, I. (1974) *Biochim. Biophys. Acta 371*, 1–13.
Itagaki, E., & Hager, L. P. (1966) *J. Biol. Chem. 241*, 3687–3695.
Jackson, J. T., La Mar, G. N., & Bartsch, R. G. (1983) *J. Biol. Chem. 258*, 1799–1805.
Jesson, J. P. (1973) in *NMR of Paramagnetic Molecules* (La Mar, G. N., Horrocks, W. D., Jr., & Holm, R. H., Eds.) pp 1–52, Academic Press, New York.
Keller, R. M., & Wüthrich, K. (1981) in *Biological Magnetic Resonance* (Berliner, L. J., & Reuben, J., Eds.) Vol. 3, pp 1–52, Plenum Press, New York.
La Mar, G. N. (1979) in *Biological Applications of Magnetic Resonance* (Shulman, R. G., Ed.) pp 305–343, Academic Press, New York.
La Mar, G. N., & Walker, F. A. (1978) in *The Porphyrins* (Dolphin, D., Ed.) Vol. IVB, pp 57–161, Academic Press, New York.
La Mar, G. N., Budd, D. B., Smith, K. M., & Langry, K. C. (1980) *J. Am. Chem. Soc., 102*, 1822–1837.
La Mar, G. N., Burns, P. D., Jackson, J. T., Smith, K. M., Langry, K. C., & Strittmatter, P. (1981) *J. Biol. Chem. 256*, 6075–6079.
La Mar, G. N., Krishnamoorthi, R., Smith, K. M. Gersonde, K., & Sick, H. (1983) *Biochemistry 22*, 6239–6246.
La Mar, G. N., Yamamoto, Y., Jue, T. Smith, K. M., & Pandey, R. K. (1985) *Biochemistry 24*, 3826–3831.
Lecomte, J. T. J., Johnson, R. D., & La Mar, G. N. (1985) *Biochim. Biophys. Acta 829*, 268–274.
Lederer, F., Glatigny, A., Bethge, P. H., Bellamy, H. D., & Mathews, F. S. (1981) *J. Mol. Biol. 148*, 427–448.
Mathews, F. S., Bethge, P. H., & Czerwinski, E. W. (1979) *J. Biol. Chem. 254*, 1699–1706.
McLachlan, S. J., La Mar, G. N., & Lee, K.-B. (1988) *Biochim. Biophys. Acta 957*, 430–435.
Meyer, T. E., & Kamen, M. D. (1982) *Adv. Protein Chem. 35*, 105–212.
Moore, G. R., & Williams, R. J. P. (1977) *FEBS Lett. 79*, 229–232.
Moore, G. R., & Williams, G. (1984) *Biochim. Biophys. Acta 788*, 147–150.
Moore, G. R., Williams, R. J. P., Peterson, J., Thomson, A. J., & Mathews, F. S. (1985) *Biochim. Biophys. Acta 829*, 83–96.
Myer, Y. P., & Bullock, P. A. (1978) *Biochemistry 17*, 3723–3729.
Nikkila, H. (1987) Ph.D. Thesis, University of Illinois.
Pande, U., La Mar, G. N., Lecomte, J. T. J., Ascoli, F., Brunori, M. Smith, K. M., Pandey, R. K., Parish, D. W., & Thanabal, V. (1986) *Biochemistry 25*, 5638–5646.
Saraiva, L. M., Liu, M. Y., Payne, W. J., Le Gall, J., Moura, J. J. G., & Moura, I. (1990) *Eur. J. Biochem. 189*, 333–341.
Satterlee, J. D. (1985) *Annu. Rep. NMR Spectrosc. 17*, 79–178.
Senn, H., & Wüthrich, K. (1983a) *Biochim. Biophys. Acta 743*, 69–81.
Senn, H., & Wüthrich, K. (1983b) *Biochim. Biophys. Acta 747*, 16–25.
Senn, H., & Wüthrich, K. (1983c) *Biochim. Biophys. Acta 746*, 48–60.
Senn, H., & Wüthrich, K. (1985) *Q. Rev. Biophys. 18*, 111–134.
Senn, H., Keller, R. M., & Wüthrich, K. (1980) *Biochem. Biophys. Res. Commun. 92*, 1362–1369.
Senn, H., Eugster, A., & Wüthrich, K. (1983) *Biochim. Biophys. Acta 743*, 58–68.
Senn, H., Guerlesquin, F., Bruschi, M., & Wüthrich, K. (1984a) *Biochim. Biophys. Acta 748*, 194–204.
Senn, H., Cusanovich, M. A., & Wüthrich, K. (1984b) *Biochim. Biophys. Acta 785*, 46–53.
Shulman, R. G., Glarum, S. H., & Karplus, M. (1971) *J. Mol. Biol. 57*, 93–115.
States, D. J., Haberkorn, R. A., & Reuben, D. J. (1982) *J. Magn. Reson. 48*, 286–292.
Takano, T., & Dickerson, R. E. (1981a) *J. Mol. Biol. 153*, 79–94.
Takano, T., & Dickerson, R. E. (1981b) *J. Mol. Biol. 153*, 95–115.
Thanabal, V., de Ropp, J. S., & La Mar, G. N. (1988) *J. Am. Chem. Soc. 109*, 7516–7525.
Timkovich, R., & Cork, M. S. (1984) *Biochemistry 23*, 851–860.
Timkovich, R., Cork, M. S., & Taylor, P. V. (1984) *J. Inorg. Biochem. 27*, 21–32.
Warme, P. K., & Hager, L. P. (1970) *Biochemistry 9*, 4244–4251.
Weber, P. C. (1982) *Biochemistry 21*, 5116–5119.
Weber, P. C., Salemme, F. R., Mathews, F. S., & Bethge, P. H. (1981) *J. Biol. Chem. 256*, 7702–7704.
Wüthrich, K. (1969) *Proc. Natl. Acad. Sci. U.S.A. 63*, 1071–1078.
Wüthrich, K. (1970) *Struct. Bonding 3*, 53–121.
Wüthrich, K. (1986) *NMR of Proteins and Nucleic Acids*, Wiley, New York.
Xavier, A. V., Czerwinski, E. W., Bethge, P. H., & Mathews, F. S. (1978) *Nature (London) 275*, 245–247.
Yu, L. P., La Mar, G. N., & Rajarathnam, K. (1990) *J. Am. Chem. Soc.* (in press).